Joint Channel Estimation and Data Detection for AFDM Receivers With Oversampling

Kuranage Roche Rayan Ranasinghe*, Yao Ge†, Giuseppe Thadeu Freitas de Abreu* and Yong Liang Guan‡
*School of Computer Science and Engineering, Constructor University, 28759 Bremen, Germany
†Continental-NTU Corporate Lab, Nanyang Technological University, 639798, Singapore
‡School of Electrical and Electronic Engineering, Nanyang Technological University, 639798, Singapore
(kranasinghe,gabreu)@constructor.university, (yao.ge,eylguan)@ntu.edu.sg

***Abstract*—In this paper, we propose a novel low complexity time domain (TD) oversampling receiver framework under affine frequency division multiplexing (AFDM) waveforms for joint channel estimation and data detection (JCEDD). Leveraging a generalized doubly-dispersive channel model, we first derive the input-output (I/O) relationship for arbitrary waveforms when oversampled in the TD and present the I/O relationship for AFDM as an example. Subsequently, utilizing the multiple sample streams created via the oversampling procedure, we use the parametric bilinear Gaussian belief propagation (PBiGaBP) technique to conduct JCEDD for decoding the transmitted data and estimating the complex channel coefficients. Simulation results verify significant performance improvements both in terms of data decoding and complex channel coefficient estimation with improved robustness against a varying number of pilots over a conventional Nyquist sampling rate receiver.**

***Index Terms*—JCEDD, AFDM, PBiGaBP, TD oversampling.**

I. Introduction

High-mobility scenarios have been a capitalizing factor driving the paradigm-shifting research for enabling the envisioned sixth-generation (6G) wireless network [1], [2], with many extended applications such as vehicle-to-everything (V2X) communications [3] and low-earth orbit (LEO) satellite networks [4]. However, the consequent fast-varying surrounding gives rise to large Doppler shifts which are commonly modelled using the doubly-dispersive channel structure [5].

Conventionally, the use of orthogonal frequency division multiplexing (OFDM) waveforms in doubly-dispersive environments results in severe degradation of communications performance [6] due to the presence of inter-carrier interference (ICI). To combat this, the orthogonal time frequency space (OTFS) waveform [7] multiplexes information symbols in the delay-Doppler (DD) domain giving it inherent robustness against ICI due to the additional degrees-of-freedom (DoF) exploited. However, due to its two-dimensional (2D) structure, OTFS incurs a much higher modulation complexity compared to OFDM. As a result, the affine frequency division multiplexing (AFDM) waveform [8] retains the same communication performance with a lower pilot overhead compared to OTFS while achieving full diversity without the higher modulation complexity due to its one-dimensional (1D) structure, making it a potential candidate for high-mobility communications.

Therefore, motivated by previous studies on oversampling receivers for the OFDM [9], [10] and OTFS [11], [12] waveforms which can further improve communication performance and robustness against fractional Doppler shifts, we consider an oversampling receiver for AFDM waveforms in high-mobility surroundings. In contrast to all the aforementioned literature which only considered data decoding with full knowledge of the complex channel coefficients (which is usually not the case) at the receiver, we now consider the joint channel estimation and data detection (JCEDD) problem, and solve it via the parametric bilinear Gaussian belief propagation (PBiGaBP) algorithm to both decode the information symbols and estimate the complex channel coefficients.

Summarizing our main contributions, we first formulate the input-output (I/O) relationship under a doubly-dispersive channel structure for arbitrary oversampled time domain (TD) signals which is then presented for AFDM. Next, using the multiple sample streams generated by the oversampling procedure, we conduct JCEDD via the PBiGaBP mechanism to extract both payload data and the complex channel coefficients with a low complexity. Finally, simulation results are presented which demonstrate a significant performance gain when an oversampled PBiGaBP receiver – which takes advantage of the larger system size due to oversampling in the belief generation stage – is used instead of a typical Nyquist rate PBiGaBP receiver. In addition, it can also be observed that the oversampling procedure increases robustness against a varying number of pilots due to the increase in factor nodes of the overall PBiGaBP framework.

II. Generalized Oversampled TD I/O Relationship

A. Doubly-Dispersive Channel Model

Utilizing the doubly-dispersive wireless channel [5], [14] to model the surrounding with one line-of-sight (LoS) and P non-LoS (NLoS) propagation paths corresponding to the P scatterers in the surrounding yields the TD channel impulse response function $h(t,\tau)$ in the continuous time-delay domain given by

$$h(t,\tau) \triangleq \sum_{p=0}^{P} h_p \cdot e^{j2\pi\nu_p t} \cdot \delta(\tau-\tau_p), \tag{1}$$

where $p = 0$ denotes the LoS path and $p \in \{1,\cdots,P\}$ corresponds to the NLoS path from each p-th scatterer; $h_p \in \mathbb{C}$ is the p-th complex fading channel coefficient; $\tau_p \in [0,\tau_{\max}]$ is the p-th path delay bounded by the maximum delay $\tau_{\max}$ and $\nu_p \in [-\nu_{\max},\nu_{\max}]$ is the p-th Doppler shift bounded by the maximum Doppler shift $\nu_{\max}$.

979-8-3315-2096-0/25/$31.00 ©2025 IEEE

B. Input-Output Relationship with TD Oversampling

Given an arbitrary baseband TD transmit signal $s(t)$ with bandwidth B, the received signal $r(t)$ after transmission over the doubly-dispersive channel $h(t,\tau)$ given in equation (1) can be described in terms of their linear convolution [5], [14]

$$\begin{aligned} r(t) &= s(t) * h(t,\tau) + w(t) \\ &\triangleq \int_{-\infty}^{+\infty} s(t-\tau)\Big(\sum_{p=0}^{P} h_p \cdot e^{j2\pi\nu_p t}\cdot\delta(\tau-\tau_p)\Big)d\tau + w(t), \end{aligned} \tag{2}$$

where $w(t)$ is the TD additive white Gaussian noise (AWGN).

Next, oversampling the TD received signal in equation (2) at an arbitrary sampling frequency $F_{\rm S} \triangleq G\cdot f_{\rm s} = \frac{G}{T_{\rm S}}$ where G is an integer oversampling factor ($i.e.$, each symbol is sampled G times), $f_{\rm S} \triangleq B$ is the typical Nyquist sampling rate (also known as the symbol-spaced sampling rate [9], [11], [12]) and $T_{\rm S}$ is the corresponding Nyquist sampling period yields [5]

$$\begin{aligned} r(nT_{\rm S}+\tfrac{g}{G}T_{\rm S}) = &\Bigg[\sum_{\ell=0}^{\infty} s(nT_{\rm S}+\tfrac{g}{G}T_{\rm S}-\ell T_{\rm S}-\tfrac{g}{G}T_{\rm S}) \\ &\times\Bigg(\sum_{p=0}^{P} h_p\cdot e^{j2\pi\nu_p(n+\frac{g}{G})T_{\rm S}}\cdot {\rm P}_{\rm RC}\big(\ell T_{\rm S}+\tfrac{g}{G}T_{\rm S}-\tau_p-\tfrac{g}{G}T_{\rm S}\big)\Bigg)\Bigg] \\ &+ w(nT_{\rm S}+\tfrac{g}{G}T_{\rm S}), \end{aligned} \tag{3}$$

where $n\in\{0,\cdots,N-1\}$ and $\ell\in\{0,\cdots,N-1\}$ denote the discrete time and delay indices, respectively; ${\rm P}_{\rm RC}$ is the raised-cosine (RC) rolloff pulse if the transmit filter response is a root raised-cosine (RRC) rolloff pulse and the receive filter is its corresponding matched filter; $g\in\{0,\cdots,G-1\}$ refers to the g-th sample stream due to oversampling and $w(nT_{\rm S}+\frac{g}{G}T_{\rm S}), \forall g$ is correlated due to the RC filter adopted (refer to Section II-C for more details on the correlation).

Since the Nyquist frequency rate $f_{\rm S}$ in typical wideband communication systems is already sufficiently high to approximate the normalized path delays $\ell_p \triangleq \tau_p f_{\rm S} = \frac{\tau_p}{T_{\rm S}} \in [0,\ell_{\max}]$ to the nearest integer with negligible error ($i.e.$, $\ell_p - \lfloor\frac{\tau_p}{T_{\rm S}}\rfloor \approx 0$) and the normalized digital Doppler shift of the p-th path is given by $f_p \triangleq \frac{N\nu_p}{f_{\rm S}} = N\nu_p T_{\rm S} \in [-f_{\max}, f_{\max}]$ [5], the RC pulses become equivalent to unit impulses due to the integer delay such that the g-th corresponding sampled sequences become

$$r^{(g)}[n] = \sum_{\ell=0}^{\infty} s[n-\ell]\Big(\sum_{p=0}^{P} h_p\cdot e^{j2\pi f_p(\frac{g+nG}{NG})}\cdot\delta[\ell-\ell_p]\Big) + w^{(g)}[n], \tag{4}$$

where $r^{(g)}[n]$, $s[n]$[1] and $w^{(g)}[n]$ are the g-th oversampled sequences of $r(t)$, $s(t)$ and $w(t)$, respectively with $\delta[\,\cdot\,]$ defined to be the discrete unit impulse function.

[1]Note that in contrast to $r^{(g)}[n]$ and $w^{(g)}[n]$, $s[n]$ does not depend on the g-th oversampled instance since the same symbol is sampled multiple times during the oversampling procedure.

Incorporating a cyclic prefix (CP) of length $N_{\rm CP}$ samples such that $N_{\rm CP} \geq \ell_{\max}$ yields

$$s[n'] = s[N+n']\cdot e^{j2\pi\phi_{\rm CP}(n')}, \tag{5}$$

where $n' \in \{-1,\cdots,-N_{\rm CP}\}$ and $\phi_{\rm CP}(n')$ is a waveform specific multiplicative phase term.

Finally, using the CP definition in equation (5) to process the linear convolution after the removal of the CP parts yields the circular convolutional form [5]

$$\mathbf{r}^{(g)} = \Big(\sum_{p=0}^{P} h_p\cdot\mathbf{\Phi}_p\cdot\big(\mathbf{\Omega}^{(g)}\big)^{f_p}\cdot\mathbf{\Pi}^{\ell_p}\Big)\cdot\mathbf{s}+\mathbf{w}^{(g)} = \mathbf{\Psi}^{(g)}\cdot\mathbf{s}+\mathbf{w}^{(g)}, \tag{6}$$

where $\mathbf{s}\in\mathbb{C}^{N\times 1}$, $\mathbf{r}^{(g)}\in\mathbb{C}^{N\times 1}$ and $\mathbf{w}^{(g)}\in\mathbb{C}^{N\times 1}$ are the transmit, received and AWGN signal vectors consisting of N samples, respectively; $\mathbf{\Psi}^{(g)}\in\mathbb{C}^{N\times N}$ is the effective circular convolutional channel matrix, $\mathbf{\Phi}_p\in\mathbb{C}^{N\times N}$ described in equation (7) is a diagonal matrix capturing the effect of the CP phase with $\phi_{\rm CP}(n)$ denoting the waveform-dependent phase function [5] on the sample index $n\in\{0,\cdots,N-1\}$; $\mathbf{\Omega}^{(g)}\in\mathbb{C}^{N\times N}$ described in equation (8) is a diagonal matrix dependent on both the g-th sampled instance and the oversampling factor G; and $\mathbf{\Pi}\in\{0,1\}^{N\times N}$ is the forward cyclic shift matrix, with elements given by

$$\pi_{i,j} = \delta_{i,j+1} + \delta_{i,j-(N-1)} \;\text{ where }\; \delta_{i,j} \triangleq \begin{cases} 0 & \text{if } i\neq j, \\ 1 & \text{if } i=j. \end{cases} \tag{9}$$

Furthermore, the roots-of-unity matrix $\mathbf{\Omega}^{(g)}$ and the forward cyclic shift matrix $\mathbf{\Pi}$ are respectively exponentiated[2] to the power of f_p and ℓ_p, which are the normalized digital Doppler frequency and the normalized delay of the p-th path.

C. Oversampled Noise Correlation Discussion

As previously discussed briefly in Section II-B, the TD AWGN vectors $\mathbf{w}^{(g)}, \forall g$ given in equation (6) are correlated as a result of oversampling each symbol [11], [12], [15].

Following [12], we denote $\mathbf{C_w}\in\mathbb{C}^{G\times G}$ to be the covariance matrix of the oversampled discrete TD AWGN vectors $\mathbf{w}^{(g)}, \forall g$ defined as

$$\mathbf{C_w} \triangleq {\rm Toepl}\Big[c_w(\frac{0}{G}),\ldots,c_w(\frac{g}{G}),\ldots,c_w(\frac{G-1}{G})\Big], \tag{10}$$

with $c_w(\frac{g}{G}) \triangleq \frac{\sigma_w^2}{2}{\rm P}_{\rm RC}(\frac{g}{G})$ where σ_w^2 is the AWGN variance and ${\rm Toepl}(\mathbf{a})$ denotes the Toeplitz matrix with elements $\mathbf{a}$.

Next, a Cholesky decomposition of $\mathbf{C_w} = \mathbf{L_C^H}\cdot\mathbf{L_C}$ yields the correlation shaping matrix $\mathbf{L_C}\in\mathbb{C}^{G\times G}$.

Finally, denoting and stacking a set of G uncorrelated AWGN noise vectors $\boldsymbol{w}_{\rm UC} \triangleq [\mathbf{w}_{\rm UC}^{(0)},\ldots,\mathbf{w}_{\rm UC}^{(g)},\ldots,\mathbf{w}_{\rm UC}^{(G-1)}]^{\mathsf{T}} \in$

[2]Matrix exponentiation of $\mathbf{\Omega}^{(g)}$ is equivalent to an element-wise exponentiation of the diagonal entries, and the matrix exponentiation of $\mathbf{\Pi}^k$ is equivalent to a forward (left) circular shift operation of k indices.

$$\mathbf{\Phi}_p \triangleq {\rm diag}\Big(\big[\overbrace{e^{-j2\pi\phi_{\rm CP}(\ell_p)},e^{-j2\pi\phi_{\rm CP}(\ell_p-1)},\ldots,e^{-j2\pi\phi_{\rm CP}(2)},e^{-j2\pi\phi_{\rm CP}(1)}}^{\ell_p\text{ terms}},\overbrace{1,1,\ldots,1,1}^{N-\ell_p\text{ ones}}\big]\Big) \in \mathbb{C}^{N\times N}. \tag{7}$$

$$\mathbf{\Omega}^{(g)} \triangleq {\rm diag}\Big(\big[e^{-j2\pi g/(NG)},e^{-j2\pi(g+G)/(NG)},\ldots,e^{-j2\pi\left(g+(N-2)G\right)/(NG)},e^{-j2\pi\left(g+(N-1)G\right)/(NG)}\big]\Big) \in \mathbb{C}^{N\times N}. \tag{8}$$

$\mathbb{C}^{G\times N}$ yields the stacked correlated AWGN noise vectors given in equation (6) to be

$$\mathbf{L_C}\cdot \boldsymbol{w}_{\rm UC} \triangleq [\mathbf{w}^{(0)},\ldots,\mathbf{w}^{(g)},\ldots,\mathbf{w}^{(G-1)}]^{\mathsf{T}} \in \mathbb{C}^{G\times N}. \quad (11)$$

III. Oversampled AFDM I/O Relationship

We consider a typical point-to-point single antenna communication system using AFDM waveforms [8], [13] composed of a transmitter and an oversampling-enabled receiver, with P significant scatterers in the environment. Using the general derivation presented in Section II for an arbitrary TD transmit signal $s(t)$, henceforth without loss of generality (w.l.g.), we consider the AFDM waveform, keeping in mind that the same logic also applies to OFDM and OTFS waveforms.

Let $\mathbf{x}\in\mathbb{C}^{N\times 1}$ denote the information vector with elements drawn from an arbitrary complex digital constellation $\mathcal{C}$, with cardinality $Q \triangleq |\mathcal{C}|$ and average symbol energy σ_X^2. The corresponding AFDM modulated transmit signal of $\mathbf{x}$ is given by its inverse discrete affine Fourier transform (IDAFT), *i.e.*,

$$\mathbf{s}_{\rm AFDM} = (\boldsymbol{\Lambda}_1^{\mathsf{H}}\mathbf{F}_N^{\mathsf{H}}\boldsymbol{\Lambda}_2^{\mathsf{H}})\cdot\mathbf{x}\in\mathbb{C}^{N\times 1}, \quad (12)$$

where $\mathbf{F}_N\in\mathbb{C}^{N\times N}$ denotes the N-point normalized discrete Fourier transform (DFT) matrix and the two diagonal chirp matrices $\boldsymbol{\Lambda}_i\in\mathbb{C}^{N\times N}$ are defined as

$$\boldsymbol{\Lambda}_i \triangleq \mathrm{diag}\Big(\big[1,\cdots,e^{-j2\pi c_i n^2},\cdots,e^{-j2\pi c_i (N-1)^2}\big]\Big), \quad (13)$$

where the first central frequency c_1 is selected for optimal robustness to doubly-dispersivity based on the channel statistics [8][3], and the second central frequency c_2 which does not depend on g can be exploited for waveform design and applications [16], [17].

In addition, the AFDM modulated signal also requires the insertion of a *chirp-periodic* prefix (CPP) to mitigate the effects of multipath propagation [8] analogous to the CP in OFDM, whose multiplicative phase function for equation (7) is given by $\phi_{\rm CPP}(n) = c_1(g)(N^2-2Nn)$ [5]. Correspondingly, the received AFDM signal vector is given by

$$\mathbf{r}_{\rm AFDM}^{(g)} \triangleq \boldsymbol{\Psi}^{(g)}\cdot\mathbf{s}_{\rm AFDM} + \mathbf{w}^{(g)} \in \mathbb{C}^{N\times 1}. \quad (14)$$

Then, the received signal in equation (14) is demodulated via the discrete affine Fourier transform (DAFT) to yield

$$\begin{aligned}\mathbf{y}_{\rm AFDM}^{(g)} &= (\boldsymbol{\Lambda}_2\mathbf{F}_N\boldsymbol{\Lambda}_1)\cdot\mathbf{r}_{\rm AFDM}^{(g)} \in \mathbb{C}^{N\times 1}\\ &= (\boldsymbol{\Lambda}_2\mathbf{F}_N\boldsymbol{\Lambda}_1)\cdot\left(\sum_{p=0}^{P} h_p\cdot\boldsymbol{\Phi}_p\cdot\left(\boldsymbol{\Omega}^{(g)}\right)^{f_p}\cdot\boldsymbol{\Pi}^{\ell_p}\right)\cdot(\boldsymbol{\Lambda}_1^{\mathsf{H}}\mathbf{F}_N^{\mathsf{H}}\boldsymbol{\Lambda}_2^{\mathsf{H}})\cdot\mathbf{x}\\ &\quad + (\boldsymbol{\Lambda}_2\mathbf{F}_N\boldsymbol{\Lambda}_1)\mathbf{w}^{(g)}. \end{aligned} \quad (15)$$

In light of the above, the final oversampled I/O relationship of AFDM over doubly-dispersive channels is given by

$$\mathbf{y}_{\rm AFDM}^{(g)} = \mathbf{G}_{\rm AFDM}^{(g)}\cdot\mathbf{x} + \tilde{\mathbf{w}}_{\rm AFDM}^{(g)} \in \mathbb{C}^{N\times 1}, \quad (16)$$

[3]Note that there are no changes to f_p due to the oversampling factor G causing no change to the corresponding effective value of c_1 and the AFDM modulation procedure.

where $\tilde{\mathbf{w}}_{\rm AFDM}^{(g)} \triangleq (\boldsymbol{\Lambda}_2\mathbf{F}_N\boldsymbol{\Lambda}_1)\mathbf{w}^{(g)} \in \mathbb{C}^{N\times 1}$ is an equivalent AWGN vector with the same statistical properties[4] as $\mathbf{w}^{(g)}$, and $\mathbf{G}_{\rm AFDM}^{(g)}\in\mathbb{C}^{N\times N}$ is the effective AFDM channel

$$\mathbf{G}_{\rm AFDM}^{(g)} \triangleq \sum_{p=0}^{P} h_p\cdot\underbrace{(\boldsymbol{\Lambda}_2\mathbf{F}_N\boldsymbol{\Lambda}_1)\cdot\left(\boldsymbol{\Phi}_p\cdot\left(\boldsymbol{\Omega}^{(g)}\right)^{f_p}\cdot\boldsymbol{\Pi}^{\ell_p}\right)\cdot(\boldsymbol{\Lambda}_1^{\mathsf{H}}\mathbf{F}_N^{\mathsf{H}}\boldsymbol{\Lambda}_2^{\mathsf{H}})}_{\boldsymbol{\Gamma}_p^{(g)}}. \quad (17)$$

IV. Joint Channel Estimation and Data Detection

In this section, the proposed JCEDD technique, termed PBiGaBP, is introduced for AFDM systems, under the general system model described in the previous section. For later convenience and effective manipulation, we now stack each g-th oversampled instance, similar to a single-input multiple-output (SIMO) scenario [11], and express the effective channel given in equation (17) in the form

$$\mathbf{y} = \begin{bmatrix}\mathbf{y}^{(0)}\\ \vdots\\ \mathbf{y}^{(g)}\\ \vdots\\ \mathbf{y}^{(G-1)}\end{bmatrix} = \sum_{p=0}^{P} h_p\cdot\underbrace{\begin{bmatrix}\boldsymbol{\Gamma}_p^{(0)}\\ \vdots\\ \boldsymbol{\Gamma}_p^{(g)}\\ \vdots\\ \boldsymbol{\Gamma}_p^{(G-1)}\end{bmatrix}}_{\boldsymbol{\Gamma}_p\in\mathbb{C}^{GN\times N}}\cdot\mathbf{x} + \underbrace{\begin{bmatrix}\tilde{\mathbf{w}}^{(0)}\\ \vdots\\ \tilde{\mathbf{w}}^{(g)}\\ \vdots\\ \tilde{\mathbf{w}}^{(G-1)}\end{bmatrix}}_{\tilde{\mathbf{w}}\in\mathbb{C}^{GN\times 1}} \in \mathbb{C}^{GN\times 1}, \quad (18)$$

with the waveform-specific subscript dropped for brevity and where the matrices $\boldsymbol{\Gamma}_p$ captures the long-term delay-Doppler statistics of the channel, which are assumed to be known[5].

Then, from equation (18), each received symbol in $\mathbf{y}$ can be described element-wise by

$$y_n = \sum_{p=0}^{P}\sum_{m=0}^{N-1} h_p\cdot\gamma_{p:n,m}\cdot x_m + \tilde{w}_n, \quad n=1,\cdots,GN, \quad (19)$$

where we slightly modify the notation formerly employed in equation (4) by denoting the m-th information symbol as x_m instead of $x[m]$, and accordingly the n-th receive signal sample by y_n instead of $y[n]$ for future clarity.

JCEDD via PBiGaBP was first introduced for AFDM systems in [13], where it was shown to outperform other alternatives like OFDM and OTFS in doubly-dispersive channels. In this paper, we show that a similar derivation can be used for oversampled AFDM systems with pertinent modifications to allow for the increased number of variable nodes.

In this manuscript, we utilize a typical AFDM frame structure, with $N_{\rm P}$ pilot symbols followed by $N-N_{\rm P}$ data symbols, as opposed to the structure with a single pilot followed by a null-guard interval considered in [21] since we do not consider a monostatic sensing scenario.

The main signal processing operations for the PBiGaBP framework used in AFDM systems is succinctly provided below. Note that all the equations are derived for a given i-th iteration of the algorithm.

[4]This is because the DAFT is a unitary transformation [8].

[5]According to [18]–[20], the delay and Doppler shifts can be assumed constant throughout multiple frame transmissions, enabling prior estimation of $\boldsymbol{\Gamma}_p, \forall p$ via radar parameter estimation (RPE) schemes using pilots [13].

1) Soft IC: For the n-th receive signal y_n given in equation (19), the soft replicas of the m-th symbol and the p-th channel gain at the $(i-1)$-th iteration of the algorithm are given by $\hat{x}_{n,m}^{(i-1)}$ and $\hat{h}_{n,p}^{(i-1)}$, respectively. With the soft replicas in hand, the corresponding mean-squared-errors (MSEs) are given by

$$\hat{\sigma}_{x:n,m}^{2(i)} \triangleq \mathbb{E}_x\big[|x-\hat{x}_{n,m}^{(i-1)}|^2\big] = E_{\mathrm{S}} - |\hat{x}_{n,m}^{(i-1)}|^2, \forall(n,m), \quad (20a)$$

$$\hat{\sigma}_{h:n,p}^{2(i)} \triangleq \mathbb{E}_h\big[|h-\hat{h}_{n,p}^{(i-1)}|^2\big] = \sigma_h^2 - |\hat{h}_{n,p}^{(i-1)}|^2, \forall(n,p), \quad (20b)$$

where $\mathbb{E}_x$ denotes the expectation over the all possible symbols x in the constellation $\mathcal{C}$, while $\mathbb{E}_h$ denotes the expectation over all possible outcomes of $h \sim \mathcal{CN}(0,\sigma_h^2)$ [13], respectively.

Next, proceeding with the soft interference cancellation (soft IC) step to compute the symbol- and channel-centric replicas $\tilde{y}_{x:m,n}^{(i)}$ and $\tilde{y}_{h:p,n}^{(i)}$ and the corresponding variances $\tilde{\sigma}_{x:m,n}^{2(i)}$ and $\tilde{\sigma}_{h:p,n}^{2(i)}$, equation (19) straightforwardly gives us

$$\tilde{y}_{x:m,n}^{(i)} = y_n - \sum_{p=0}^{P}\sum_{q\neq m}^{N-1} \hat{h}_{n,p}^{(i-1)} \cdot \gamma_{p:n,q} \cdot \hat{x}_{n,q}^{(i-1)}. \quad (21)$$

Exploiting the fact that $\tilde{y}_{x:m,n}^{(i)}, \forall m,n$ follow Gaussian probability density functions (PDFs) and defining $\mathrm{y}_n, \forall n$ to be an auxiliary variable, the soft IC symbol replicas are defined as

$$\tilde{y}_{x:m,n}^{(i)} \sim p_{\mathrm{y}_n|x_m}(\mathrm{y}_n|x_m) \propto \exp\!\left(-\frac{|\mathrm{y}_n - \tilde{\gamma}_{x:m,n}^{(i)} x_m|^2}{\tilde{\sigma}_{x:m,n}^{2(i)}}\right), \quad (22)$$

with $\tilde{\gamma}_{x:m,n}^{(i)}, \forall m,n$ implicitly denoting the corresponding soft IC effective channel gains given by

$$\tilde{\gamma}_{x:m,n}^{(i)} \triangleq \sum_{p=0}^{P} \hat{h}_{n,p}^{(i-1)} \gamma_{p:n,m}, \quad (23)$$

while the soft IC conditional variances $\tilde{\sigma}_{x:m,n}^{2(i)}$ are approximated by replacing the instantaneous values with the long-term statistics as

$$\begin{aligned}\tilde{\sigma}_{x:m,n}^{2(i)} &\triangleq \mathbb{E}_{x,h}\big[|\tilde{y}_{x:m,n}^{(i)} - \tilde{\gamma}_{x:m,n}^{(i)} x_m|^2\big] \\ &\approx \sum_{p=0}^{P} \hat{\sigma}_{h:n,p}^{2(i-1)} |\hat{y}_{x_m:n,p}^{(i)}|^2 + \sum_{q\neq m}^{N-1} \hat{\sigma}_{x:n,q}^{2(i-1)} |\tilde{\gamma}_{x:q,n}^{(i)}|^2 + N_0 + \\ &\sum_{p=0}^{P} \hat{\sigma}_{h:n,p}^{2(i-1)} \sum_{q\neq m}^{N-1} \hat{\sigma}_{x:n,q}^{2(i-1)} |\gamma_{p:n,q}|^2 + E_{\mathrm{S}} \sum_{p=0}^{P} \hat{\sigma}_{h:n,p}^{2(i-1)} |\gamma_{p:n,m}|^2, \quad (24)\end{aligned}$$

where the received signal estimate $\hat{y}_{x_m:n,p}^{(i)}$ after cancellation of the m-th soft symbol estimate is given by

$$\hat{y}_{x_m:n,p}^{(i)} \triangleq \sum_{q\neq m}^{N-1} \gamma_{p:n,q} \hat{x}_{n,q}^{(i-1)}. \quad (25)$$

In a similar fashion, the channel-centric replica can also be expressed as

$$\tilde{y}_{h:p,n}^{(i)} = y_n - \sum_{q\neq p}^{P} \hat{h}_{n,q}^{(i)} \cdot \hat{y}_{h:n,q}^{(i)}, \quad (26)$$

with the corresponding variance given by

$$\begin{aligned}\tilde{\sigma}_{h:p,n}^{2(i)} &\triangleq \sum_{q\neq p}^{P} \hat{\sigma}_{h:n,q}^{2(i-1)} |\hat{y}_{h:n,q}^{(i)}|^2 + \sum_{m=0}^{N-1} \hat{\sigma}_{x:n,m}^{2(i-1)} |\tilde{\gamma}_{h_p:m,n}^{(i)}|^2 + N_0 + \\ &\sum_{q\neq p}^{P} \hat{\sigma}_{h:n,q}^{2(i)} \sum_{m=0}^{N-1} \hat{\sigma}_{x:n,m}^{2(i)} |\gamma_{q,nm}|^2 + \sigma_h^2 \sum_{m=0}^{N-1} \hat{\sigma}_{x:n,m}^{2(i)} |\gamma_{p:n,m}|^2, \quad (27)\end{aligned}$$

where the channel-centric soft channel estimate $\hat{y}_{h:n,p}^{(i)}$ and the corresponding soft IC effective channel gain of the p-th path $\tilde{\gamma}_{h_p:m,n}^{(i)}$ are respectively defined as

$$\hat{y}_{h:n,p}^{(i)} \triangleq \sum_{m=0}^{N-1} \gamma_{p:n,m} \hat{x}_{n,m}^{(i-1)} \text{ and } \tilde{\gamma}_{h_p:m,n}^{(i)} \triangleq \sum_{q\neq p}^{P} \hat{h}_{n,q}^{(i-1)} \gamma_{q,nm}. \quad (28)$$

2) Belief Generation: Beginning with the assumption that $G \cdot N \cdot P$ is a large enough scalar and that the individual estimation errors in $\hat{h}_{n,p}^{(i-1)}$ and $\hat{x}_{n,q}^{(i-1)}$ are uncorrelated, scalar Gaussian approximation (SGA) can be applied to generate the beliefs of all the symbols by substituting equation (19) into (21) to obtain the belief corresponding to the m-th symbol x_m at the n-th factor node by combining the contributions of all signals in $\mathbf{y}$, excluding y_n, as

$$p_{\mathrm{x}|x_m}(\mathrm{x}|x_m) = \prod_{q\neq n}^{N} p_{\mathrm{y}_q|\mathrm{x}_m}(\mathrm{y}_q|x_m) \propto \exp\!\left(-\frac{|\mathrm{x}-\tilde{x}_{n,m}^{(i)}|^2}{\tilde{\sigma}_{\tilde{x}:n,m}^{2(i)}}\right), \quad (29)$$

to extract the desired beliefs and their variances following

$$\tilde{x}_{n,m}^{(i)} \triangleq \tilde{\sigma}_{\tilde{x}:n,m}^{2(i)} \sum_{q\neq n}^{N} \frac{\tilde{\gamma}_{x:m,q}^{*(i)} \tilde{y}_{x:m,q}^{(i)}}{\tilde{\sigma}_{x:m,q}^{2(i)}} \text{ and } \tilde{\sigma}_{\tilde{x}:n,m}^{2(i)} \triangleq \left(\sum_{q\neq n}^{N} \frac{|\tilde{\gamma}_{x:m,q}^{(i)}|^2}{\tilde{\sigma}_{x:m,q}^{2(i)}}\right)^{-1}. \quad (30)$$

Similarly, the extrinsic beliefs of the channel gains can be modelled under SGA by the approximate distribution

$$p_{\mathrm{h}|h_p}(\mathrm{h}|h_p) \propto \exp\!\left(-\frac{|\mathrm{h}-\tilde{\mathrm{h}}_{n,p}^{(i)}|^2}{\tilde{\sigma}_{\tilde{\mathrm{h}}:n,p}^{2(i)}}\right), \quad (31)$$

to extract the desired beliefs and their variances following

$$\tilde{\mathrm{h}}_{n,p}^{(i)} \triangleq \tilde{\sigma}_{\tilde{\mathrm{h}}:n,p}^{2(i)} \sum_{q\neq n}^{N} \frac{\hat{y}_{h:qp}^{*(i)} \tilde{y}_{h:p,q}^{(i)}}{\tilde{\sigma}_{h:p,q}^{2(i)}} \text{ and } \tilde{\sigma}_{\tilde{\mathrm{h}}:n,p}^{2(i)} \triangleq \left(\sum_{q\neq n}^{N} \frac{|\hat{y}_{h:qp}^{(i)}|^2}{\tilde{\sigma}_{h:p,q}^{2(i)}}\right)^{-1}. \quad (32)$$

3) Soft Replica Generation: Finally, once again exploiting SGA and explicitly defining $p_{\mathrm{x}|x}\big(\mathrm{x}|x;\tilde{x}_{n,m}^{(i)},\tilde{\sigma}_{\tilde{x}:n,m}^{2(i)}\big)$ and $p_{\mathrm{h}|h}\big(\mathrm{h}|h;\tilde{h}_{n,p}^{(i)},\tilde{\sigma}_{\tilde{h}:n,p}^{2(i)}\big)$ to be the likelihood functions of the data symbols and channel beliefs given in equations (29) and (31), respectively, the soft replicas of x_m and h_p can be obtained from the conditional expectation given the extrinsic beliefs as

$$\hat{x}_{n,m}^{(i)} = \frac{\sum_{x\in\mathcal{C}} x \cdot p_{\mathrm{x}|x}\big(\mathrm{x}|x;\tilde{x}_{n,m}^{(i)},\tilde{\sigma}_{\tilde{x}:n,m}^{2(i)}\big) \cdot p_x(x)}{\sum_{x'\in\mathcal{C}} p_{\mathrm{x}|x'}\big(\mathrm{x}|x';\tilde{x}_{n,m}^{(i)},\tilde{\sigma}_{\tilde{x}:n,m}^{2(i)}\big) \cdot p_{x'}(x')}, \quad (33)$$

$$\hat{h}_{n,p}^{(i)} = \frac{\int h \cdot p_{\mathrm{h}|h}\big(\mathrm{h}|h;\tilde{h}_{n,p}^{(i)},\tilde{\sigma}_{\tilde{h}:n,p}^{2(i)}\big) \cdot p_h(h)}{\int p_{\mathrm{h}|h'}\big(\mathrm{h}|h';\tilde{h}_{n,p}^{(i)},\tilde{\sigma}_{\tilde{h}:n,p}^{2(i)}\big) \cdot p_{h'}(h')}. \quad (34)$$

Next, under the assumption that each element x of the data vector is independently drawn with equal probability out of Q-points contained in the constellation $\mathcal{C}$ and the prior $p_x(x)$ is

Algorithm 1 Proposed PBiGaBP-based JCEDD Technique for Oversampled AFDM Systems in Doubly-Dispersive Channels

Input: demodulated receive signal $\mathbf{y}$, pilot symbols $\mathbf{x}_p$, DD matrices $\mathbf{\Gamma}_p$, constellation power E_S, noise variance N_0, channel variance per path σ_h^2 and damping factors β_x and β_h.
Output: decoded symbols $\mathbf{x}_d$ and channel estimates $\hat{h}_p, \forall p$.

Initialization
- Set iteration counter to $i = 0$ and amplitudes $c_x = \sqrt{E_\mathrm{S}/2}$
- Fix pilots to $\hat{x}_{n,m}^{(i)} = [\mathbf{x}_p]_m$ and set corresponding variances to $\hat{\sigma}_{x:n,m}^{2(i)} = 0, \forall n, m \in \mathcal{M}_p$
- Set initial data and channel estimates to $\hat{x}_{n,m}^{(0)}$=0 and $\hat{h}_{n,p}^{(0)}$=0 and corresponding variances to $\hat{\sigma}_{x:n,m}^{2(0)} = E_\mathrm{S}, \forall n, m \in \mathcal{M}_d$ and $\hat{\sigma}_{h:n,p}^{2(0)} = \sigma_h^2, \forall n, p$, respectively.

for $i = 1$ to $i_{\max}$ **do**
Channel Estimation: $\forall n, p$
1: Compute the variables $\tilde{y}_{h:n,p}^{(i)}$ and $\tilde{\gamma}_{h_p:m,n}^{(i)}$ from eq. (28).
2: Compute soft signal $\tilde{y}_{h:p,n}^{(i)}$ and its corresponding variance $\tilde{\sigma}_{h:p,n}^{2(i)}$ from equation (26) and equation (27), respectively.
3: Compute extrinsic channel belief $\tilde{h}_{n,p}^{(i)}$ and its corresponding variance $\tilde{\sigma}_{\tilde{h}:n,p}^{2(i)}$ from equation (32).
4: Compute denoised and damped channel estimate $\hat{h}_{n,p}^{(i)}$ and its corresponding variance $\hat{\sigma}_{h:n,p}^{2(i)}$ from equation (38) and equation (39), respectively.
Data Detection: $\forall n, m$
5: Compute auxiliary variables $\tilde{\gamma}_{x:m,n}^{(i)}$ and $\hat{y}_{x_m:n,p}^{(i)}$ from equations (23) and (25), respectively.
6: Compute soft signal $\tilde{y}_{x:m,n}^{(i)}$ and its corresponding variance $\tilde{\sigma}_{x:m,n}^{2(i)}$ from equation (21) and equation (24), respectively.
7: Compute extrinsic data belief $\tilde{x}_{n,m}^{(i)}$ and its corresponding variance $\tilde{\sigma}_{\tilde{x}:n,m}^{2(i)}$ from equation (30).
8: Compute denoised and damped data estimate $\hat{x}_{n,m}^{(i)}$ and its corresponding variance $\sigma_{x:n,m}^{2(i)}$ from equations (35) and (36) and equations (20a) and (37), respectively.
end for

a Multinomial distribution of the Q-th order, the beliefs $\hat{x}_{n,m}^{(i)}$ can be explicitly computed for quadrature phase-shift keying (QPSK) modulated symbols via

$$\hat{x}_{n,m}^{(i)} = c_x \cdot \left(\tanh\left[2c_x \frac{\Re\{\tilde{x}_{n,m}^{(i)}\}}{\tilde{\sigma}_{\tilde{x}:n,m}^{2(i)}} \right] + j \tanh\left[2c_x \frac{\Im\{\tilde{x}_{n,m}^{(i)}\}}{\tilde{\sigma}_{\tilde{x}:n,m}^{2(i)}} \right] \right), \quad (35)$$

where $c_x \triangleq \sqrt{E_\mathrm{S}/2}$ denotes the magnitude of the real and imaginary parts of the explicitly chosen QPSK symbols.

To further improve convergence [22], the final output is computed by damping the result $\hat{x}_{n,m}^{(i)}$ from equation (35) with a damping factor $0 < \beta_x < 1$ to yield

$$\hat{x}_{n,m}^{(i)} = \beta_x \hat{x}_{n,m}^{(i)} + (1 - \beta_x) \hat{x}_{n,m}^{(i-1)}, \quad (36)$$

with its corresponding variance $\hat{\sigma}_{x:n,m}^{2(i)}$ also updated and damped following equation (20a) to give

$$\hat{\sigma}_{x:n,m}^{2(i)} = \beta_x (E_\mathrm{S} - |\hat{x}_{n,m}^{(i)}|^2) + (1 - \beta_x) \hat{\sigma}_{x:n,m}^{2(i-1)}. \quad (37)$$

Similarly, notice that the likelihood in equation (34) is a Gaussian-product distribution, with the mean of $p_h(h)$ equal to zero [23]. Therefore, the channel estimate belief can be straightforwardly computed and damped with a damping factor $0 < \beta_h < 1$ via

$$\hat{h}_{n,p}^{(i)} = \beta_h \frac{\sigma_h^2 \tilde{h}_{n,p}^{(i)}}{\tilde{\sigma}_{\tilde{h}:n,p}^{2(i)} + \sigma_h^2} + (1 - \beta_h) \hat{h}_{n,p}^{(i-1)}, \quad (38)$$

and

$$\hat{\sigma}_{h:n,p}^{2(i)} = \beta_h \frac{\sigma_h^2 \tilde{\sigma}_{\tilde{h}:n,p}^{2(i)}}{\tilde{\sigma}_{\tilde{h}:n,p}^{2(i)} + \sigma_h^2} + (1 - \beta_h) \hat{\sigma}_{h:n,p}^{2(i-1)}. \quad (39)$$

The proposed PBiGaBP-based JCEDD algorithm is summarized as a pseudocode in Algorithm 1.

V. Simulation Results

A. Numerical Simulations

We consider an oversampled millimeter-wave (mmWave) [13], [24] AFDM system at $G = 2$ consisting of $N = 128$

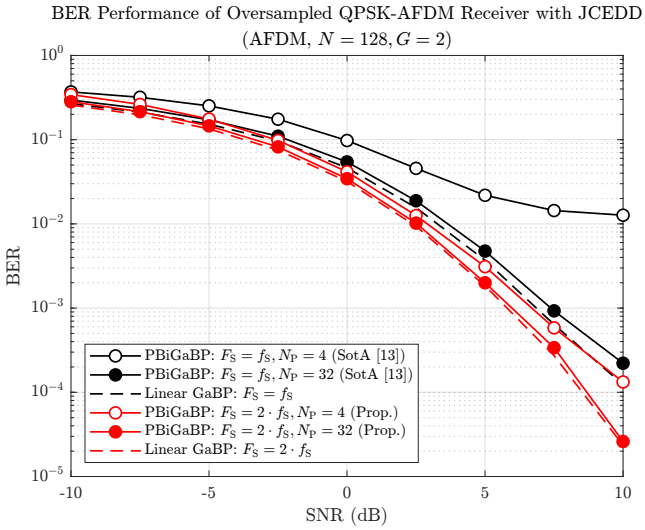

(a) BER Performance.

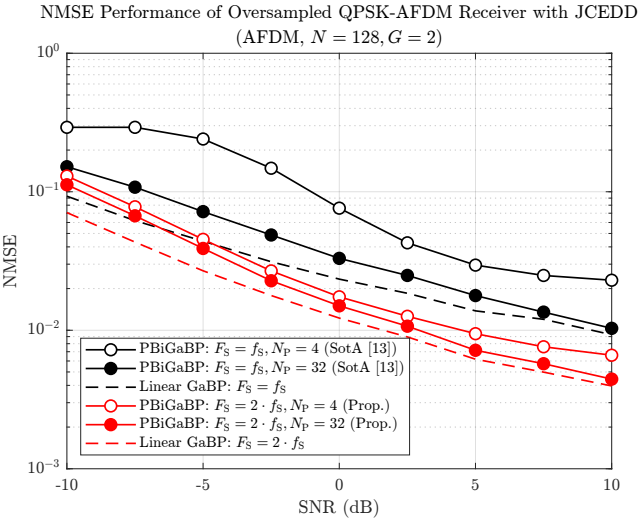

(b) NMSE Performance.

Fig. 1. Performance of the proposed oversampled AFDM receiver via the PBiGaBP algorithm compared to the SotA Nyquist receiver under a varying number of N_P pilots.

subcarriers with 1 LoS path and 4 NLoS paths ($i.e., P = 4$) operating at 70 GHz with a bandwidth of 20 MHz using QPSK symbols. For the doubly-dispersive channel model, we consider a maximum unambiguous range of 75 m and a maximum unambiguous velocity of 602 km/h, which gives us a maximum normalized delay index of 20 and a maximum normalized digital Doppler shift index of 0.25 (i.e., $\ell_{\max} = \frac{\tau_{\max}}{T_{\mathrm{S}}} = 20$ and $f_{\max} = N\nu_{\max}T_{\mathrm{S}} = 0.25$). The path delays τ_p are then randomly generated using a uniform distribution across $[0, \tau_{\max}]$ and Jakes' Doppler spectrum [8] is used for the generation of the path Dopplers as $\nu_p = \nu_{\max}\cos(\theta_p)$, where θ_p is uniformly distributed over $[-\pi, \pi]$. W.l.g., P_{RC} in equation (3) is also simplified to a sinc filter, which corresponds to a RC pulse with a rolloff factor 0. Regarding the PBiGaBP algorithm, we set $\beta_x, \beta_h = 0.3$, the maximum number of iterations $i_{\max} = 40$, the constellation power $E_{\mathrm{S}} = 1$ and the average channel power per path $\sigma_h^2 = 1$.

Proceeding by using the Linear Gaussian belief propagation (GaBP)[6] as a lower bound, we compare in Fig. 1 the communications and CE performances, in terms of bit error rate (BER) and normalized mean square error (NMSE), respectively, achieved by PBiGaBP employed by the oversampled AFDM receiver with $G = 2$.

The results show that the proposed oversampled PBiGaBP-based JCEDD with AFDM outperforms a system employing the same PBiGaBP technique but using a SotA Nyquist rate receiver, both in terms of BER with a 2.5 dB gain and NMSE with a 5 dB gain. In addition, we observe that the proposed receiver has an improved robustness to the change in the number of pilots with minimal performance degradation compared to the SotA as seen from Fig. 1, even when the pilot symbol percentage is changed from 25% (32 pilots) to 3.125% (4 pilots) due to the increase in factor nodes.

B. Complexity Analysis

Considering the typical floating point operations performed, the computational complexity of the proposed PBiGaBP algorithm for oversampled systems is $\mathcal{O}(N^2G(P+1))$ which is linear on the number element-wise operations executed. This is therefore of a much lower complexity than the compared Linear GaBP method which incurs a total computational complexity of $\mathcal{O}(N^3)$ due to the costly matrix inversion carried out during the channel estimation procedure.

VI. Conclusion

In this paper, we examined the JCEDD performance of an oversampled AFDM system in a doubly-dispersive surrounding. By deriving a general TD oversampling model for arbitrary waveforms, we present the oversampled AFDM case as an example. Then, we numerically verify that the proposed TD oversampling mechanism yields significant performance gains, both in terms of BER and NMSE performance. Finally, we reveal that oversampling significantly improves the robustness of the system against a varying number of pilots, given that the performance deviation is minimum even when the number of pilot symbols are reduced significantly.

[6]An estimation method that uses GaBP for both channel estimation (CE) (with full knowledge of symbols) and data decoding (with full knowledge of channel coefficients), via an linear minimum mean square error (LMMSE) initialization for CE. This provides a lower bound on the performance for the proposed method in exchange for a large computational cost.

Acknowledgement

This work was supported in part by the RIE2020 Industry Alignment Fund-Industry Collaboration Projects (IAF-ICP) Funding Initiative, as well as cash and in-kind contribution from the industry partner(s).

References

[1] J. Wu *et. al*, "A Survey on High Mobility Wireless Communications: Challenges, Opportunities and Solutions," *IEEE Access*, vol. 4, 2016.
[2] W. Jiang *et. al*, "The Road Towards 6G: A Comprehensive Survey," *IEEE Open J. Commun. Soc.*, vol. 2, 2021.
[3] S. Chen *et. al*, "Vehicle-to-Everything (V2X) Services Supported by LTE-Based Systems and 5G," *IEEE Communications Standards Magazine*, vol. 1, no. 2, 2017.
[4] J. Shi *et. al*, "OTFS Enabled LEO Satellite Communications: A Promising Solution to Severe Doppler Effects," *IEEE Net.*, vol. 38, no. 1, 2024.
[5] H. S. Rou *et. al*, "From OTFS to AFDM: A Comparative Study of Next-Generation Waveforms for ISAC in Doubly-Dispersive Channels [Special Issue on Sig. Proc. for the Integrated Sensing and Communications Revolution]," *IEEE Sig. Proc. Mag.*, vol. 41, no. 5, Nov. 2024.
[6] T. Wang *et. al*, "Performance degradation of OFDM systems due to Doppler spreading," *IEEE Trans. Wireless Commun.*, vol. 5, no. 6, 2006.
[7] R. Hadani *et. al*, "Orthogonal Time Frequency Space Modulation," in *IEEE Wireless Comm. and Networking Conference (WCNC)*, 2017.
[8] A. Bemani, N. Ksairi, and M. Kountouris, "Affine Frequency Division Multiplexing for Next Generation Wireless Communications," *IEEE Trans. Wireless Commun.*, vol. 22, no. 11, 2023.
[9] Q. Shi *et. al*, "Fractionally Spaced Frequency-Domain MMSE Receiver for OFDM Systems," *IEEE Trans. Veh. Technol.*, vol. 59, no. 9, 2010.
[10] J. Wu and Y. R. Zheng, "Oversampled Orthogonal Frequency Division Multiplexing in Doubly Selective Fading Channels," *IEEE Trans. Commun.*, vol. 59, no. 3, 2011.
[11] Y. Ge *et. al*, "Receiver Design for OTFS with a Fractionally Spaced Sampling Approach," *IEEE Trans. Wireless Comm.*, vol. 20, no. 7, 2021.
[12] P. Priya *et. al*, "Low Complexity MRC Detection for OTFS Receiver With Oversampling," *IEEE Trans. Wireless Comm.*, vol. 23, no. 2, 2024.
[13] K. R. R. Ranasinghe *et. al*, "Joint Channel, Data, and Radar Parameter Estimation for AFDM Systems in Doubly-Dispersive Channels," *IEEE Transactions on Wireless Communications*, 2024.
[14] D. W. Bliss and S. Govindasamy, *Dispersive and doubly dispersive channels*. Cambridge University Press, 2013, pp. 341–364.
[15] S. Kay, *Intuitive Probability and Random Processes using MATLAB*. Berlin, Heidelberg: Springer-Verlag, 2007.
[16] J. Zhu *et. al*, "A low-complexity radar system based on affine frequency division multiplexing modulation," *arXiv:2312.11125*, 2023.
[17] H. S. Rou *et. al*, "AFDM Chirp-Permutation-Index Modulation with Quantum-Accelerated Codebook Design," *arXiv preprint arXiv:2405.02085*, 2024.
[18] G. Matz, "On non-WSSUS wireless fading channels," *IEEE Trans. Wireless Commun.*, vol. 4, no. 5, 2005.
[19] H. B. Mishra *et. al*, "OTFS Channel Estimation and Data Detection Designs with Superimposed Pilots," *IEEE Trans. Wireless Commun.*, vol. 21, no. 4, 2022.
[20] X. Yang *et. al*, "Sensing Aided Uplink Transmission in OTFS ISAC With Joint Parameter Association, Channel Estimation and Signal Detection," *IEEE Trans. Veh. Technol.*, vol. 73, no. 6, 2024.
[21] A. Bemani *et. al*, "Integrated Sensing and Communications with Affine Frequency Division Multiplexing," *IEEE Wireless Commun. Lett.*, 2024.
[22] Q. Su and Y.-C. Wu, "On Convergence Conditions of Gaussian Belief Propagation," *IEEE Trans. Signal Process.*, vol. 63, no. 5, 2015.
[23] J. T. Parker *et. al*, "Bilinear Generalized Approximate Message Passing—Part I:Derivation," *IEEE Trans. Signal Process.*, vol. 62, no. 22, 2014.
[24] H. Wymeersch *et. al*, "Integration of Communication and Sensing in 6G: a Joint Industrial and Academic Perspective," in *IEEE 32nd Annual Int. Symp. on Personal, Indoor and Mobile Radio Comm. (PIMRC)*, 2021.